Biocatalytic Self-Assembly Cascades

Jugal Kishore Sahoo,*[a, e] Charalampos G. Pappas,[a, b] Ivan Ramos Sasselli,[a] Yousef M. Abul-Haija [a] and Rein V. Ulijn*[a, b, c, d]

Abstract: *The properties of supramolecular materials are dictated by both kinetic and thermodynamic aspects, providing opportunities to dynamically regulate morphology and function. In here, we demonstrate time dependent regulation of supramolecular self-assembly by connected, kinetically competing enzymatic reactions. Starting from Fmoc-tyrosine phosphate and phenylalanine amide in the presence of an amidase and phosphatase, four distinct self-assembling molecules may be formed which each give rise to distinct morphologies (spheres, fibers, tubes/tapes and sheets). By varying the sequence or ratio in which the enzymes are added to mixtures of precursors, these structures can be (transiently) accessed and interconverted. The approach provides insights into dynamic self-assembly using competing pathways that may aid the design of soft nanostructures with tunable dynamic properties and life times.*

Supramolecular self-assembly[1a-e] provides a powerful approach for the discovery and development of functional nanostructures. The emphasis in this area is increasingly focused on non-equilibrium aspects of structure formation, including chemically fueled assembly,[2]spatial control of assembly in patterns,[3]mechano-responsive pathway selection [4] or (bio-)catalytic self-assembly.[5]Supramolecular order is dictated not only bymolecular design but also by the pathway of assembly,[6-9]which may be controlled by (temporary) changes in environment, such as pH[9], solvent composition, [10-12] catalyst concentrations[8], by modifications in molecular (linker) design.[13]

Biocatalytic self-assembly *i.e.* the enzymatic activation of precursors of supramolecular building blocks, provides an attractive approach to controlling the kinetics of supramolecular structure formation under constant, physiological conditions.[8,14]Biocatalytic self-assembly may proceed under thermodynamic control, where the assembled product is reversibly formed and thermodynamically favored,[16] orit may proceed under kinetic control, where the product remains trapped in local minima in the energy landscape[8] or exists transiently as a result of competing assembly and dis-assembly pathways.[2a] The use of multiple enzymes in competing assembly and dis-assembly reactions has previously been demonstrated, giving rise to dynamic regulation of fiber formation.[15a-c]

In here, we demonstrate that distinct supramolecular structures can be accessed from a single pool of precursors that serve as substrates for connected biocatalytic pathways, where the product of the first enzymatic reaction is consumed by the second one and *vice versa*. Very recently, Bing Xu's group demonstrated dynamic regulation of fiber formation using a phosphatase/esterase pair to influence cancer cell fate.[15d]

Specifically, the system involves two different enzymes that catalyze competing reactions (**Figure 1**): alkaline phosphatase (ALP) and an amidase (thermolysin). The former dephosphorylates tyrosine phosphate, as previously demonstrated in biocatalytic self-assembly[14] while the later catalyzes(reversible)amide hydrolysis and condensation.[16] The reactants, which are precursors of aromatic peptide amphiphiles,[17]were selected for their previously reported differences in nanoscale morphology upon self-assembly: spheres for 9-fluorenyl methyloxycarbonyl-tyrosine (Fmoc-Y*p*-OH),[18]fibers for Fmoc-Y-OH[14a,18], tubes/tapes for Fmoc-Y*p*F-NH_2 and sheets for Fmoc-YF-NH_2.[20]Three pathways were explored involving either, sequential enzyme addition (Pathways *I* and *II*) or one-pot system where both enzymes are present but their ratios were varied (*Pathway III*) (**Figure 1**).

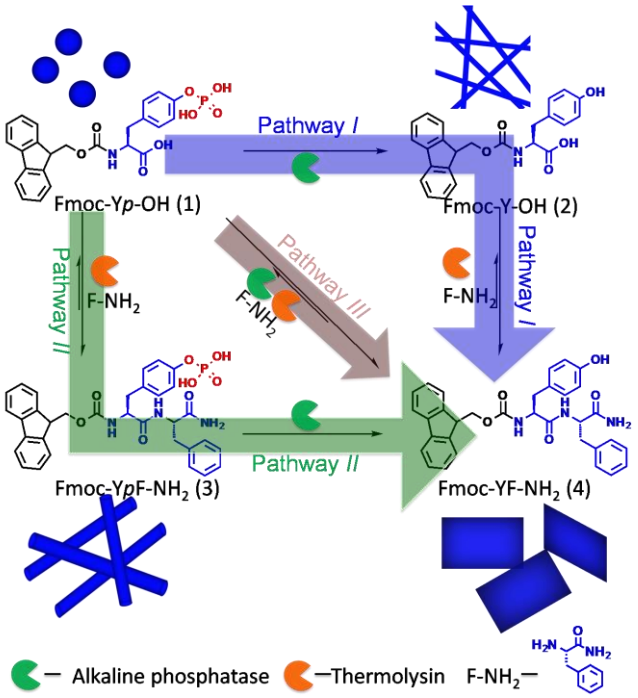

Figure 1. Schematicrepresentation of sequential ((blue and green arrows, Pathways*I* and *II*)and competing (brown arrow, Pathway *III*) biocatalytic pathways from precursorsFmoc-Y*p*-OH and F-NH_2.

[a] Dr.Jugal Kishore Sahoo, Dr.Charalampos G. Pappas, Dr. Ivan Ramos Sasselli, Dr.Yousef M. Abul-Haija, and Prof. Rein V. Ulijn
Department of Pure and Applied Chemistry, Technology and Innovation Centre, University of Strathclyde, Glasgow, UK
E-mail: jsahoo@nd.edu, Rein.Ulijn@asrc.cuny.edu
[b] Advanced Science Research Center (ASRC), City University of New York, 85 St Nicholas Terrace, New York, New York 10031, USA.
[c] Hunter College, Department of Chemistry, Hunter College, CUNY, 695 Park Avenue, New York, New York 10065, USA.
[d] Chemistry and Biochemistry programs, The Graduate Center of the City University of New York, New York, NY 10016, USA.
[e] Department of Chemical and Biomolecular Engineering, University of Notre Dame, Notre Dame, IN 46556, USA

Supportinginformationforthisarticleisgiven via a link atthe end ofthedocument.

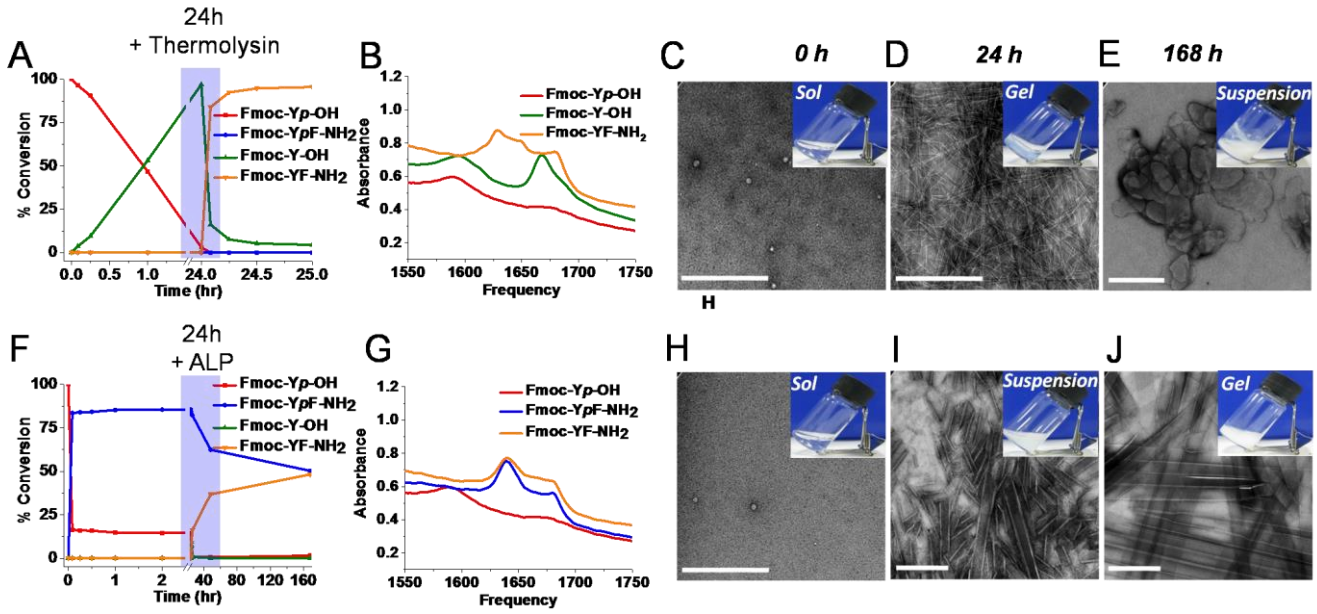

Figure 2. Spectroscopic and microscopic analysis of biocatalytic self-assembly cascades through different pathways: A, F) HPLC data of time-dependant formation of various supramolecular intermediates, involved in *Pathway I* and *II*. B, G) FT-IR spectra at different time points involving biocatalytic *Pathway I* and *II*. Fmoc-Y-OH after 24h of ALP addition in Pathway *I*and Fmoc-YF-NH_2 after 168h of thermolysin addition in Pathway *I*; In Pathway *II*, Fmoc-YpF-NH_2 (blue line) after 24h of thermolysin addition and Fmoc-YF-NH_2 (mixture; orange line) after 168h of ALP addition. C, D, E) Transmission electron microscopic images of the supramolecular intermediates involved in *PathwayI* at time points 0h, 24h and 168h of enzyme exposure respectively. H, I, J) corresponding electron microscopic images of *PathwayII* at different time points.Figure insets represent digital images of respective macroscopic appearances of the corresponding supramolecular structures (Scale Bar- 500 nm).

The first objective was to demonstrate that both enzymes can act *in tandem* so that different nanoscale morphologies could be accessed. In *Pathway I*, the first step is de-phosphorylation of Fmoc-Y*p*-OH to Fmoc-Y-OH which was monitored by high pressure liquid chromatography (HPLC), showing a near-complete conversion (96 %) after 24h (**Figure 2A,** *green line*). A macroscopic transition could be observed from solution (Fmoc-Y*p*-OH; 20mM) to a self-supporting hydrogel (Fmoc-Y-OH) (**Figure 2C**and **2D***inset,* **Figure S1**) coinciding with a nanosphere (approximately 20-30nm in diameter) to twisted nanofiber transition as observed by Transmission electron microscope (TEM) (micrometers in length and 20-30 nm in diameter)[14](**Figure 2D, S3A, B, C**). After 24h, thermolysin and 80 mM F-NH_2 were added which gave rise to formation of a milky suspension (**Figure 2E** *inset,* **Figure S1**), corresponding to near-complete conversion (95%) to Fmoc-YF-NH_2 (**Figure 2A**, *orange line*). Fmoc-YF-NH_2 forms a sheet-like morphology (**Figure 2E, S3 D, E, F**).[20]

The supramolecular(re)-organization of Fmoc- moieties was monitored using fluorescence spectroscopy. In the de-phosphorylation step, we observe a reduced relative intensity of the peak around 380 nm, which is due to the loss of micelle like structure (**Figure S2**).[21] Fourier-transform infrared spectroscopy (FT-IR) was performed to investigate the changes in H-bonding patterns (**Figure 2B**) for *Pathway I*. A peak at 1670 cm^{-1}arises upon the formation of Fmoc-Y-OH due to formation of H-bonded stacks of the carbamate groups.[23] Both of these show another broad peak below 1600 cm^{-1} caused by a portion of deprotonated carboxylic C-terminus.[24]Therefore, the dephosphorylation gives a loss of the π-stacking while favoring H-bonding, suggesting that a balance of both dictates supramolecular order. The subsequent formation of Fmoc-YF-NH_2 gives rise to a red-shift of the 320 nm fluorescence emission, suggesting enhanced overlap of Fmoc-groups and a broad feature composed of a series of further red-shifted broad peaks between 380 and 600 nm, indicating formation of higher order aggregates (**Figure S2**).The FT-IR shows that the condensation of Fmoc-Y-OH and F-NH_2 to form Fmoc-YF-NH_2 gives rise to two different amide vibrations: at 1625 cm^{-1} and at 1650 cm^{-1}, and the increment in frequency of the carbamate vibration. Both types of vibrations are in typical frequencies for H-bonded amide groups in Fmoc-dipeptide based nanostructures.[23] The shift of the carbamate to higher frequencies (1680 cm^{-1}) is likely to be due to a destabilization of the carbamate arrangement to favor the incorporation of the amide groups to the H-bonded stacks. Thus, the FT-IR shows that the amide bond formation modifies the H-bonding arrangement, probably to accommodate the new π-stacking interactions shown with the fluorescence and the new H-bonds of the amide group. The FT-IR spectra of the enzymes and precursor (F-NH_2) is provided in supporting information (**Figure S10**).

In *Pathway II*, the sequence of addition of enzymes is reversed. Thermolysin first catalyzes the amide condensation reaction in presence of F-NH_2 to give rise to 84% Fmoc-Y*p*F-NH_2 (**Figure 2F;** *blue line*).[20] Macroscopically, it forms a milky suspension immediately upon thermolysin addition (**Figure 2I***inset,* **S4B**). After adding ALP, it is evident that the de-phosphorylation

reaction is relatively slow and eventually reaches 48% of Fmoc-YF-NH_2 (**Figure 2F**, *orange line*) after one week. It is likely that the observed slow kinetics are related to sterically hindered accessibility of the phosphate groups in the assembled state of Fmoc-Y*p*F-NH_2. A macroscopic transition from the suspension state to an opaque, self-supporting gel is observed (**Figure 2J** *inset,* **S4C**). TEM shows a tube-or tape-like morphology for Fmoc-Y*p*F-NH_2 after 24h (**Figure 2I, S6 A, B, C**) and subsequently, the mixture of Fmoc-Y*p*F-$NH_2$and Fmoc-YF-NH_2gives rise to larger structures which appear to be a combination of tubes and 2D tapes (**Figure 2J, S6D, E, F**). It should be noted that the sheet-like morphology of Fmoc-YF-NH_2 is not observed in *Pathway II*, however the observation of tapes supports that 2D assemblies become more favored upon Fmoc-Y*p*F-NH_2de-phosphorylation.

Fluorescence spectroscopy reveals a red-shift of the Fmoc-moiety (323 nm; **Figure S5B**) after 24h, indicating aggregation [23]and increase in supramolecular order upon formation of Fmoc-Y*p*F-NH_2. Upon addition of ALP, an increase in relative peak intensity at 468nm is observed, which is associated with formation of extended Fmoc-stacks enabled by formation of Fmoc-YF-NH_2(**Figure S5B**). Analysis of *Pathway II* by FT-IR (**Figure 2G**) shows a similar carbamate peak at 1680 cm^{-1} and amide peak at 1640 cm^{-1} for both Fmoc-Y*p*F-NH_2 (after 24h) and Fmoc-YF-NH_2 after 1 week of enzyme exposure. This observation suggests that, while the condensation modifies the H-bonding in *Pathway II*, the de-phosphorylation is in this case not as important for the H-bonding as it was as first step in *Pathway I*.

Having established that four distinct morphologies can be accessed when using this combination of enzymes and precursors (spheres for Fmoc-Y*p*-OH, fibers for Fmoc-Y-OH, tubes/tapes for Fmoc-Y*p*F-NH_2, sheets for Fmoc-YF-NH_2 and a combination of longer tubes and tapes for Fmoc-Y*p*F-NH_2/Fmoc-YF-NH_2), we subsequently introduced both enzymes at the same time at varying ratios of 1:1, 1:10, 1:20 and 1:100 thermolysin/ALP (*Pathway III*) (keeping the phosphatase concentration fixed at 50U). The concentration details of ratios of both enzymes are provided in **Table S1** and digital images showing macroscopic appearance at different time points in **Figure S7**.

When both enzymes were present at the activities used in the 'sequential' experiments (1:1), the system is first dominated by thermolysin activity, giving rise to 85% conversion to Fmoc-Y*p*F-NH_2 in 5 minutes, (similar to *Pathway II*) which subsequently starts de-phosphorylating and form 56% of Fmoc-YF-NH_2 after 1 week (**Figure 3A;** *orange line*). The overall HPLC profile resembles that of the sequential enzyme addition experiment (**Figure 2F**) but shows faster kinetics that are likely related to enhanced access of the phosphate group due to dynamic hydrolysis/condensation of the amide bond. In TEM, we observe a mixture of nanotubes and 2D tape-like morphology after 1 week of enzyme exposure (**Figure 3F, S8A, B, C**), which resembles the final morphology observed in *Pathway II*.

At 1:10, simultaneous de-phosphorylation and condensation reactions are also observed, however it is clear that the higher thermolysin concentration favors amide bond formation prior to de-phosphorylation. The final composition of different supramolecular products after 1 week (Fmoc-Y*p*F-NH_2(48%), Fmoc-YF-NH_2 (47%)) (**Figure 3B**), where Fmoc-YF-$NH_2$is formed mostly by de-phosphorylation of Fmoc-Y*p*F-NH_2. This is also reflected in the transmission electron microscopy, where nanotube/sheet-like structures dominate (**Figure 3G, S8 D, E, F**).

With lower thermolysin concentration (1:20), the reaction clearly undergoes competing condensation and de-phosphorylation (**Figure 3C**) where we observe a mixture of all components with Fmoc-Y-OH and Fmoc-Y*p*F-NH_2formed approximately at equal rates during the first 2 hours (**Figure 3E**). After 2h, we observe a decrease in Fmoc-Y-OH, as it achieved a concentration sufficient to favor direct formation of Fmoc-YF-NH_2 *via* condensation with F-NH_2. After 1 week, Fmoc-YF-NH_2, formed by condensation of Fmoc-Y-OH and de-phosphorylation of Fmoc-Y*p*F-NH_2, dominates (55%) and a mixture of sheets, fibers and tubular morphologies are observed (**Figure 3H**, **S8 G, H, I)**. While final molecular compositions are similar for these three enzyme concentrations, the morphologies observed are different (tapes/tubes;tubes;sheets/tubes) which relates to the pathways of formation involving dramatic differences in relative concentrations of the transient intermediates Fmoc-Y and Fmoc-Y*p*F-NH_2 (0.5/76; 15/57; 40/34) after 2h of exposure at enzyme ratios 1:1, 1:10 and 1:20 respectively.

At the lowest thermolysin concentration (1:100), the supramolecular transition initially resembles *Pathway I.*The initial stage of self-assembly is controlled by ALP (**Figure3E**), as can be seen with the formation of Fmoc-Y-OH, which is followed by simultaneous condensation of to lower levels of Fmoc-Y*p*F-NH_2 and Fmoc-YF-NH_2. The final composition of supramolecular products after 1 week is Fmoc-Y-OH (65%), Fmoc-Y*p*F-NH_2 (11%) and Fmoc-YF-NH_2 (24%) (**Figure 3D**).This ratio of products is reflected in the supramolecular morphology observed by TEM where we observe twisted nanofibers due to Fmoc-Y-OH and long tape (2D) and tubular structures typical for Fmoc-YF-NH_2 and Fmoc-Y*p*F-NH_2(**Figure 3I, S8 J, K, L**).

FT-IR spectroscopic study for all concentrations of thermolysin (**Figure S9**) was performed to show the presence of H-bonding and stacking in the formation of supramolecular structures. In each case, we observe similar final spectra, with carbamate peak at 1680 cm^{-1} and amide peak at 1640 cm^{-1}.

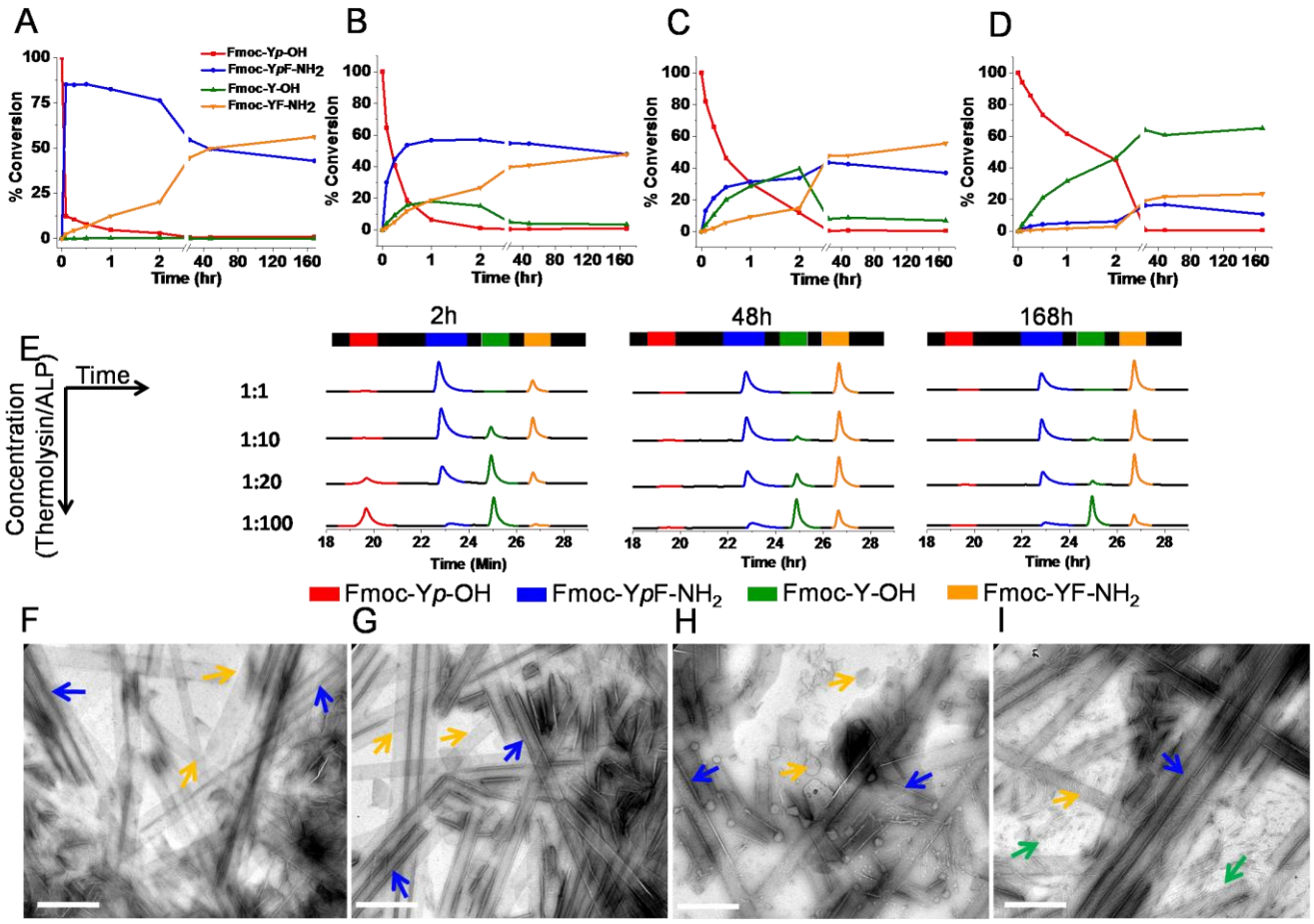

Figure 3. Supramolecularbiocatalytic transformations observed in direct competition with ALP and thermolysin present in *Pathway III*. HPLC (A, B, C, D) time course at different ratios of thermolysin and ALP; A) 1:1 B) 1:10; C) 1:20; D)1:100. E) Represents the HPLC chromatogram for all different concentration ratios of enzymes at different time points to show the self-assembly kinetics observed at different concentrations. F, G, H, I) Represents the electron microscopy images after 1 week of enzyme exposure in the order of thermolysin concentrations in A, B, C, D respectively. Color arrows in the images represent corresponding peptide nanostructures(Scale bar- 1 µm)

In summary, we have demonstrated a biocatalytic self-assembly cascade where, by using two biocatalysts in different sequence and ratios, the structure, composition and morphology of the structures formed could be dynamically regulated. This approach should be applicable for exploring supramolecular assemblies where pathway dictates structure and function.[25,15b]In addition, the use of competing enzymes performing *in tandem* without affecting each other's function, paves the way to more complex supramolecular polymerizations.

Acknowledgements

We thank BBSRC for funding (BB/Koo7513/1). The research leading to these results has received funding from the European Research Council under European Union's Seventh Framework Programme (FP7/2007-2013)/ERC grant agreement number 258775and US Air Force (AFOSR, grant FA9550-15-1-0192). IRS acknowledges financial support from the EC 7th Framework Programme Marie Curie Actions via the European ITN SMARTNET No. 316656.

Keywords: Biocatalysis• Enzyme cascade• Supramolecular chemistry• Pathway selection• Aromatic peptide amphiphile

[1] a) J-M. Lehn, *Science*, **2002**, *295*, 2400-2403; b) G. Whitesides, B. Grzybowski, *Science*, **2002**, *295*, 2418-2421; c) E. Mattia, S. Otto, *Nat. Nanotechnol*.**2015**, *10*, 111-119; d) T. Aida, E. W. Meijer, S. I. Stupp, *Science*, **2012**, *335*, 813-817; e) M. J. Webber, E. A. Appel, E. W. Meijer, R. Langer, *Nat. Mater*.**2016**, *15*, 13-26.

[2] a) C. G. Pappas, I. R. Sasseli, R. V. Ulijn, *Angew. Chem. Int. Ed*. **2015**, *54*, 8119-8123; b) T. Heuser, E. Weyandt,A. Walther, *Angew. Chem. Int. Ed.* **2015**, *54*, 13258-13262; c) J. Boekhoven, W. E. Hendriksen, G. J. M. Koper, R. E. Eelkema, J. H. van Esch, *Science*, **2015**, *349*, 1075-1079; d) I. R. Epstein, B. Xu, *Nat. Nanotechnol*, **2016**, *11*, 312-319; e) B. A. Grzybowski, W. T. S. Huck, *Nat. Nanotechnol*.**2016**, *11*, 585-592.

[3] a) E. R. Draper, E. G. B. Eden, T. O. McDonald, D. J. Adams, *Nat. Chem*. **2015**, *7*, 848-852; b) D. J. Cornwell, B. O. Okesola, D. K. Smith, *Angew. Chem. Int. Ed*. **2014**, *53*, 12461-12465.

[4] a) C. G. Pappas, T. Mutasa, P. W. J. M. Frederix, S. Fleming, S. Bai, S. Debnath, S. M. Kelly, A. Gachagan, R. V. Ulijn, *Mater. Horiz*. **2015**, *2*, 198-202; b) J. M. A. Carnall, C. A. Waudby, A. M. Belenguer, M. C. A. Stuart, J. J.-P. Peyralans, S. Otto, *Science*, **2010**, *327*, 1502-1506.

[5] a) F. Trausel, F. Versluis, C. Maity, J. M. Poolman, M. Lovrak, J. H. Van Esch, R. Eelkema, *Acc. Chem. Res.***2016,***49*, 1440-1447; b) J. K. Sahoo, S. K. M. Nalluri, N. Javid, H. Webb, R. V. Ulijn, *Chem. Commun*. **2014**, *50*, 5462-5464; c) R. Haburcak, J. Shi, X. Du, D. Yuan, B. Xu, *J. Am. Chem. Soc*. **2016**, *138*, 15397-15404.

[6] P. A. Korevaar, S. J. George, A. J. Markvoort, M. M. J. Smulders, P. A. J. Hilbers, A. P. H. J. Schenning, T. F. A. DeGreef, E. W. Meijer, *Nature*, **2012**, *481*, 492-497.

[7] J. Boekhoven, J. M. Poolman, C. Maity, F. Li, L. van der Mee, C. B. Minkenberg, E. Mendes, Jan H. van Esch, R. Eelkema, *Nat. Chem*. **2013,***5*, 433-437.

[8] A. R. Hirst, S. Roy, M. Arora, A. K. Das, N. Hodson, P. Murray, S. Marshall, N. Javid, J. Sefcik, J. Boekhoven, Jan H. van Esch, S. Santabarbara, N. T. Hunt, R. V. Ulijn, *Nat. Chem*. **2010**, *2*, 1089-1094.

[9] J. Raeburn, A. Z. Cardoso, D. J. Adams, *Chem. Soc. Rev*., **2013**, *42*, 5143-5156.

[10] a) P. Jonkheijm, P. van der Schoot, A. P. H. J. Schenning, E. W. Meijer, *Science*, **2006**, *313*, 80-83; b) P. A. Korevaar, C. J. Newcomb, E. W. Meijer, S. I. Stupp, *J. Am. Chem. Soc.***2014**, *136 (24)*, 8540-8543; c) G. Leonetti, S. Otto, *J. Am. Chem. Soc*. **2015**, *137*, 2067-2072.

[11] J. Wang, K. Liu, L. Yan, A. Wang, S. Bai, X. Yan, *ACS Nano*, **2016**, *10 (2)*, 2138-2143.

[12] P. A. Korevaar, T. F. A. de Greef, E. W. Meijer, *Chem. Mater.***2014**, *26 (1)*, 576-586.

[13] S. Ogi, V. Stepanenko, J. Thein, F. Würthner,*J. Am. Chem. Soc.* **2016**, *138*, 670-678.

[14] a) Z. Yang, H. Gu, D. Fu, P. Gao, J. K. Lam, B. Xu, *Adv. Mater.***2004**, *16*, 1440-1444.b) H. Kühnle, H. G. Börner, *Angew. Chem. Int. Ed*., **2009**, *48 (35)*, 6431-6434.

[15] a) A. K. Das, R. Collins, R. V. Ulijn, *Small*, **2008**, *4 (2)*, 279-287;b) Z.Yang, G. Liang, L. Wang, B. Xu. *J. Am. Chem. Soc.*, **2006**, *128*, 3038–3043; c) M.J. Webber, C.J. Newcomb, R. Bitton, S.I. Stupp, *Soft Matter***2011**,*7*, 9665-9672.d) Z. Feng, H. Wang, R. Zhou, J. Li, B. Xu, *J. Am. Chem. Soc*., **2017**, 139 (11), 3950-3953.

[16] R.J. Williams, A.M. Smith, R. Collins, N. Hodson, A.K. Das, R.V. Ulijn,*Nat.Nanotechnol.*, **2009**, *4*, 19-24.

[17] a) K. Tao, A. Levin, L. A.- Abramovich, E. Gazit, *Chem. Soc. Rev*. **2016**, *45***,** 3935-3953;b) Y. Zhang, H. Gu, Z. Yang, B. Xu, *J. Am. Chem. Soc*. **2003**, *125 (45)*, 13680-13681.; c) S. Fleming, R. V. Ulijn, *Chem. Soc. Rev.* **2014**, *43*, 8150-8177; d) I.W. Hamley, *Angew. Chem. Int. Ed.* 46, 8128-8147; e) D.M. Ryan, B.L. Nilsson, *Polym. Chem.***2012**, *3*, 18–33.

[18] K. Thornton, Y. M. Abul-Haija, N. Hodson, R. V. Ulijn, *Soft Matter*, **2013**, *9*, 9430-9439.

[19] J. Gao, H. Wang, L. Wang, J. Wang, D. Wang, Z. Wang, *J. Am. Chem. Soc.***2009**, *131*, 11286-11287.

[20] C. G. Pappas, Y. M. Abul-Haija, A. Flack, P. W. J. M. Frederix, R. V. Ulijn, *Chem. Commun*. **2014**, *50*, 10630-10633.

[21] Y. M. Abul-Haija, S. Roy, P. W. J. M. Frederix, N. Javid, V. Jayawarna, R. V. Ulijn, *Small***2014**, *10*, 973-979.

[22] Y. Hong, J. W. Y. Lam, B. Z. Tang, *Chem. Soc. Rev*. **2011**, *40*, 5361-5388.

[23] S. Fleming, P.W.J.M. Frederix, I. Ramos-Sasselli, N. Hunt, R.V. Ulijn and T. Tuttle, *Langmuir*, **2013**, 29, 9510-9515.

[24] A. K. Ghosh, V. N. Viswanadhan, J. J. Wendoloski, *J. Phys. Chem. A***1998**, *102*, 3762-3772.

[25] J. Zhou, X. Du, N. Yamagata, B. Xu, *J. Am. Chem. Soc*. **2016**, *138*, 3813-3823.